AN EXTENDED DYNAMIC MODEL OF A GEYSER INDUCED BY AN INFLOW OF GAS (2): EFFECTS OF VARIOUS SHAPES AND REPEATED EXPANSIONS AND CONTRACTIONS IN AN UNDERGROUND WATERCOURSE

H Kagami

Dept of Preschool Education, Nagoya College, 48 Takeji, Sakae-cho, Toyoake, Aichi, 470-1193, Japan
Email: kagami@nagoyacollege.ac.jp

ABSTRACT

We modified further our extended dynamic model of a geyser induced by an inflow of gas, by taking into consideration the effects during spouting of an elbow shape, pairs of sudden expansions and contractions, and repeats of this shape in an underground watercourse. Through numerical simulations of this extended dynamic model, we see that a large number of sudden expansions and contractions or a large angular elbow in the underground watercourse greatly affects the spouting dynamics of the geyser.

Keywords: Geyser, Inflow of gas, Model, Numerical simulation, Elbow, Sudden expansion, Sudden contraction, Watercourse, Spouting dynamics, Application

1 INTRODUCTION

Geysers are classified into two types dependent upon the inducer: the first type is induced by boiling, and the other is induced by an inflow of gas (a periodic bubbling spring). Boiling induced geysers are very common throughout the world. Theories about this type of geyser's mechanisms have been proposed (Honda & Terada, 1906), and the application of these theories to other phenomena has also been discussed (Lorenz, 2002). Also, observational studies of these geysers exist (Husen et al., 2004). On the other hand, gas induced geysers are found very infrequently and have been the subject of only a few studies (Iwasaki, 1962). Our study focuses on these latter geysers. Iwasaki (1962) did model experiments of a geyser induced by an inflow of gas and showed that the injection of higher pressure gas caused the water to spout intermittently. He calculated spouting time and pause time using the gas supply rate as a parameter based on a mathematical model of gas balance. However, his model did not discuss the spouting dynamics.

Thus, we proposed a mathematical model (a static model) (Kagami et al., 2000; Kagami, 2006) and a dynamic model (Kagami, 2002, 2006) of a geyser induced by an inflow of gas based on observation (Ishii et al., 1999) and model experiments of the Hirogawara Geyser (Yamagata, Japan) (Katase et al., 1999) so as to reproduce its spouting dynamics. Then through modifying the dynamic model many times (Kagami, 2003; 2007), we proposed a model combining the above two models (Kagami, 2006). Numeric simulations of the modified dynamic, the combined, and the modified models show the recurrent dynamics of geyser spouting (periodic bubbling springs). It is possible to estimate the parameters (volume of the underground space, depth of spouting hole, and so on) under a geyser by comparing the results of simulation with those of observation (Kagami, 2003; 2006; 2009). Moreover, we have verified the above models through geological exploration, analysis of hot spring water, and radioactive prospecting (Kagami, 2007).

However, in the case of the above models, it was assumed for simplicity that the underground watercourse was vertically straight even though it is expected that an underground watercourse has a complicated shape in the deep underground regions. Each of these complicated shapes creates resistance. Therefore, to the results of our former study, we have added two main effects – the sudden expansion and the sudden contraction of the watercourse within the various shapes it may take. We have discussed these effects quantitatively through numerical simulation of the extended model (Kagami, 2007), in which we supposed that the watercourse had one sudden expansion and one sudden contraction.

In reality, however, the watercourses may have various shapes. Because it is obvious that these complex shapes in a watercourse have a complex effect on the spouting dynamics of the geyser, we must add these effects and those of repeats of these shapes in a watercourse to the former model so as to better re-create the spouting

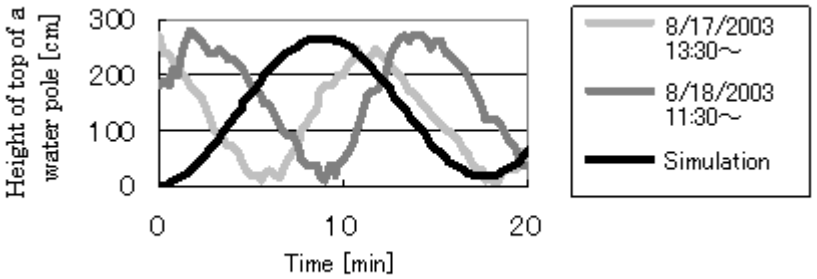

Figure 1. A graph of the numerical simulation of Equation (2) compared with observations of a geyser induced by an inflow of gas (Kibedani geyser in Yamagata, Japan) (Kagami, in press).

dynamics of this type of geyser and estimate the underground parameters more accurately.

In this study, we expand further our expanded model through adding the effects of an elbow shape and repeats of the same shape in a watercourse during spouting to the combined model and estimate their effects on the spouting dynamics through numerical simulation of the further extended model.

2 MODEL

First, we describe the outlines of the three models (dynamic, mathematic or static, and combined) and introduce their most important results. Then we present the derivation of the extended dynamic model to which the above-mentioned effects were added and the major results of its numeric simulation. Finally, we introduce the further extended model, that is, the application of the extended dynamic model to an elbow shape and repeats of the same shape in the watercourse and give the results of the numeric simulation.

2.1 The former models

Because a detailed derivation of the three original models of a gas inflow induced geyser was already presented in former papers (Kagami 2003, 2006), we show here only the outlines and main findings.

In cases where the friction between the walls of a spouting pipe and the water packed in it has not been taken into account, an evolutionary equation of temporal variations of the height of the top of a water pole packed in the spouting pipe of a periodic bubbling spring is written as:

$$(n_0+\beta t)(V_0+Sx)\rho H\frac{d^3x}{dt^3}+(n_0+\beta t)pS\frac{dx}{dt}=(V_0+Sx)p\beta \tag{1}$$

where n_0 represents the molar amount of gas in an underground space just before the water pole begins to rise up to the upper entrance of the spouting pipe; β is a constant concerning the gas supply rate; V_0 represents the volume of gas packed in a underground cave; S represents the area of a cross section of the spouting pipe; H represents the length (height) of a small volume of water packed in the pipe; p represents the pressure of the gas packed in the underground cave; and x is the position of the lower interface between the water and the gas in the water pole. An upper direction of a vertical line is regarded as the plus direction of the x-axis. A detailed derivation of Equation (1) is shown in the Appendix

In cases where the friction between the walls of a spouting pipe and water packed in it has been taken into account, Equation (1) is changed to Equation (2).

$$(n_0+\beta t)(V_0+Sx)\rho H\frac{d^3x}{dt^3}+\frac{8\pi\eta H}{S}(n_0+\beta t)(V_0+Sx)\frac{d^2x}{dt^2}+(n_0+\beta t)pS\frac{dx}{dt}=(V_0+Sx)p\beta \tag{2}$$

where η represents the viscosity coefficient. As a result, the second term of Equation (2) is added and represents the effects of viscosity.

A sample of a numerical simulation of Equation (2) is shown in Figure 1(Kagami, in press). In the graph, the numerical simulation of Equation (2) is compared with the observational results. We can guess the underground parameters that cannot be measured easily because of geological difficulties.

Using the mathematical (static) model, a spouting period τ is represented as a function of various parameters. For example, a spouting period τ can be written as:

$$\tau = \frac{V_0}{\alpha\beta} + \frac{f_k S}{\rho g \alpha\beta}\left(f_k + P_0 + \rho g H\right) \tag{3}$$

where $\alpha = RT$; R represents the gas constant; T represents temperature; f_k represents pressure due to surface tension on the interface between the water packed in the spouting pipe and the gas in the underground cave; P_0 represents atmospheric pressure; and g represents gravity acceleration. For example, when we observe a spouting period of a geyser induced by an inflow of gas, we can evaluate the underground parameters (volume of the underground space (V_0), depth of spouting hole (H), and so on) through Equation (3).

The combined model unites the dynamic and the mathematical models. The combined model enables us to find a more reliable estimation of the underground parameters of this type of geyser because the dynamic model's method of estimating underground parameters is independent of that of the mathematical model.

2.2 The extended dynamic model

In the extended dynamic model, we took into consideration the effects of a pair of sudden expansions and contractions as would occur in a complicated underground watercourse, as it is thought that these sudden expansions and contractions are frequently observed in underground watercourses and their resistance is comparatively large.

Sudden expansion and sudden contraction are shown in Figures 2 and 3, respectively. D_1 and D_2 in each figure represent the diameters of the wide and narrow parts of a pipe respectively. V_1 and V_2 represent the velocity of the flows in each part. The shape of a sudden expansion is the same as one of sudden contraction as shown in both figures. However, in the case of sudden expansion, water flows from a narrow part of the pipe to a wide one, while in a contraction, water flows from a wide part of the pipe to a narrow one. For example, if hot spring water passes a sudden contraction region when it flows upward, the region replaces a sudden expansion region when it flows downward.

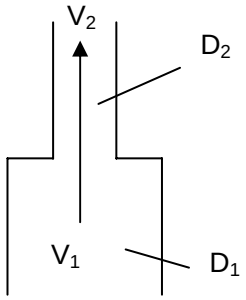

Figure 2. Illustration of a sudden contraction

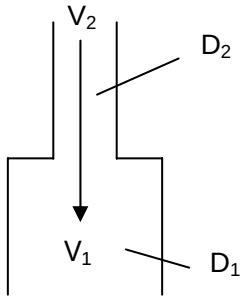

Figure 3. Illustration of a sudden expansion

The loss water head of sudden expansion h_{se} and that of sudden contraction h_{sc} are defined using the loss coefficient of sudden expansion f_{se} and that of sudden contraction f_{sc} respectively as:

$$h_{se} = f_{se}\frac{V_1^{\,2}}{2g} \tag{4}$$

$$h_{sc} = f_{sc} \frac{V_2^{\,2}}{2g} = f_{sc} \left(\frac{D_1}{D_2} \right)^4 \frac{V_1^{\,2}}{2g} \tag{5}$$

where g represents gravity acceleration.

Now we assume the direction from a wide part of the pipe to a narrow one, that is, the direction of an up-pointing arrow in Figure 2 coincides with the vertically upward direction. A spouting mode begins when the surface tension on the interface between the water packed in the spouting pipe and the gas in the underground cave (and weight of a small volume of water packed in the spouting pipe and pressure of the atmosphere) becomes smaller than the pressure of gas in the underground cave. Then an equation of motion of the small volume of water is written as (Kagami, 2003):

$$\rho SH \frac{d^2 x}{dt^2} = pS - \rho gSH - p_0 S \tag{6}$$

where x is regarded as the position of the lower interface between the water and gas in the water pole, and the upper direction of a vertical line is regarded as a plus direction of the x-axis. Adding the effects of a sudden contraction and expansion to the former model in Equation (6), we get the following equations.

(1) In the case of $\frac{dx}{dt} \geq 0$

$$\rho SH \frac{d^2 x}{dt^2} = pS - \rho gSH - p_0 S - \rho gSh_{sc} \tag{7}$$

(2) In the case of $\frac{dx}{dt} \leq 0$

$$\rho SH \frac{d^2 x}{dt^2} = pS - \rho gSH - p_0 S - \rho gSh_{se} \tag{8}$$

Finally, we arrive at the following equations to replace Equation (1).

(1) In the case of $\frac{dx}{dt} \geq 0$

$$(n_0 + \beta t)(V_0 + Sx)\rho H \frac{d^3 x}{dt^3} + (n_0 + \beta t)(V_0 + Sx)\rho f_{sc} \frac{dx}{dt} \frac{d^2 x}{dt^2} + (n_0 + \beta t) pS \frac{dx}{dt} = (V_0 + Sx) p\beta \tag{9}$$

(2) In the case of $\frac{dx}{dt} \leq 0$

$$(n_0 + \beta t)(V_0 + Sx)\rho H \frac{d^3 x}{dt^3} + (n_0 + \beta t)(V_0 + Sx)\rho f_{se} \left(\frac{D_2}{D_1} \right)^4 \frac{dx}{dt} \frac{d^2 x}{dt^2} + (n_0 + \beta t) pS \frac{dx}{dt} = (V_0 + Sx) p\beta \tag{10}$$

Equations (9) and (10) are basic equations that include the effects of a sudden contraction and expansion.

2.3 The further extended dynamic model (application of the former extended dynamic model)

In this section, we expand the former dynamic model into the case where a shape, for example, an elbow shape, or repeats of the same shape, for example, repeats of a sudden contraction and expansion, exist in a watercourse.

2.3.1 The case where repeat pairs of sudden contractions and expansions exist in a watercourse

In the case where repeats of the same shapes exist in a watercourse, we can easily modify the former extended dynamic model by taking the effects of these repeats into consideration. For example, in the case where repeat pairs of sudden contractions and expansions exist in a watercourse, the extended dynamic model is modified as

follows.

(1) In the case of $\frac{dx}{dt} \geq 0$

$$(n_0 + \beta t)(V_0 + Sx)\rho H \frac{d^3x}{dt^3} + (n_0 + \beta t)(V_0 + Sx)\rho m f_{sc} \frac{dx}{dt}\frac{d^2x}{dt^2} + (n_0 + \beta t)pS\frac{dx}{dt} = (V_0 + Sx)p\beta \quad (11)$$

(2) In the case of $\frac{dx}{dt} \leq 0$

$$(n_0 + \beta t)(V_0 + Sx)\rho H \frac{d^3x}{dt^3} + (n_0 + \beta t)(V_0 + Sx)\rho m f_{se} \left(\frac{D_2}{D_1}\right)^4 \frac{dx}{dt}\frac{d^2x}{dt^2} + (n_0 + \beta t)pS\frac{dx}{dt} = (V_0 + Sx)p\beta \quad (12)$$

where m represents the number of repeats of pairs of sudden contractions and expansions. Equations (11) and (12) are basic equations that include these effects.

2.3.2 The case where an elbow shape exists in a watercourse

When a shape exists in a watercourse, we can easily modify the extended dynamic model, taking the effects of the shape into consideration. For example, we consider an elbow shape in a watercourse, as illustrated in Figure 4. The arrow shows the flow, which is turned at the region resembling a human elbow.

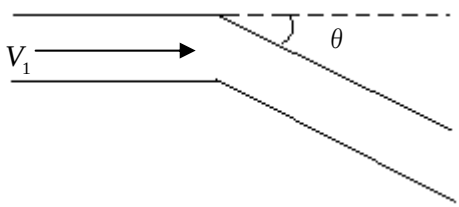

Figure 4. Illustration of an elbow shape

The loss water head of elbow h_b is written using the loss coefficient of the elbow f_b as:

$$h_b = f_b \frac{V_1^2}{2g} \quad (13)$$

where V_1 represents the velocity of the flow. The loss coefficient of elbow f_b is experimentally written using an angle ϑ of the elbow as:

$$f_b = 0.946\sin^2\frac{\vartheta}{2} + 2.05\sin^4\frac{\vartheta}{2} \quad (14)$$

Thus, in the case where an elbow shape exists in a watercourse, the extended dynamic model is modified as follows.

(1) In the case of $\frac{dx}{dt} \geq 0$

$$(n_0 + \beta t)(V_0 + Sx)\rho H \frac{d^3x}{dt^3} + (n_0 + \beta t)(V_0 + Sx)\rho f_b \frac{dx}{dt}\frac{d^2x}{dt^2} + (n_0 + \beta t)pS\frac{dx}{dt} = (V_0 + Sx)p\beta \quad (15)$$

(2) In the case of $\frac{dx}{dt} \leq 0$

$$(n_0 + \beta t)(V_0 + Sx)\rho H \frac{d^3x}{dt^3} + (n_0 + \beta t)(V_0 + Sx)\rho f_b \frac{dx}{dt}\frac{d^2x}{dt^2} + (n_0 + \beta t)pS\frac{dx}{dt} = (V_0 + Sx)p\beta \quad (16)$$

Equations (15) and (16) are basic equations that include the effects of an elbow shape.

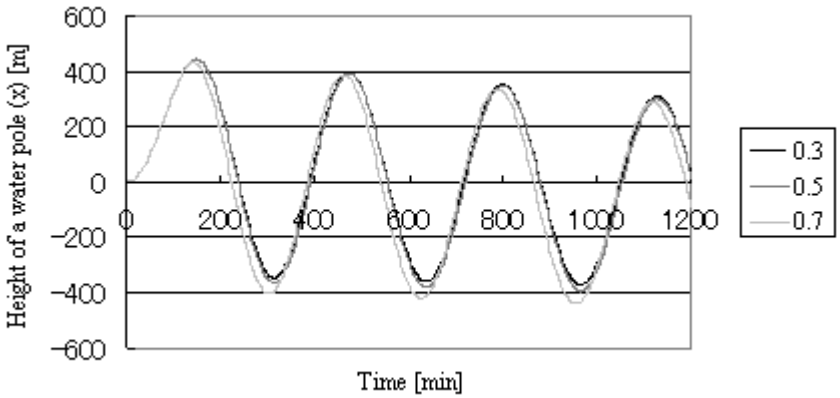

Figure 5. Temporal variation at the top of a water pole depends on the ratio of D_2: D_1

3 RESULTS AND DISCUSSION

In this section, we show the results of numerical simulation of the extended dynamic model and the further extended dynamic model and discuss the models by comparing these results. The following parameter values are common to both models: $V_0 = 9.90\times10^{5}\left[m^3\right]$, $\rho = 1.00\times10^{3}\left[kg/m^3\right]$, $g = 9.80\times10^{0}\left[kg\cdot m/s^2\right]$, $H = 1.00\times10^{2}\left[m\right]$, $\beta = 1.90\times10^{-4}\left[mol/s\right]$, and $S = 1.00\times10^{-2}\left[m^2\right]$. n_0 is calculated using Equation (26) when $p_0 = 1.01\times10^{5}[Pa]$ and $f_k = 2.20\times10^{1}[N/m^2]$. Each model equation is simulated numerically using the Runge-Kutta method.

Based on observational results, it has been determined that the gas slug in the underground space (see Figure 8 in the Appendix) never reaches the spouting exit (Figure 8) during the spouting of water packed in the pipe (Ishii et al., 1999). Also, the gas slug never breaks the interface between the water packed in the spouting pipe and the gas in the underground space (Figure 8) when at least a cross section of the spouting pipe is very small (Kagami, 2002). On the other hand, the effects of a loss of a part of the water packed in the spouting pipe due to its spouting have already been discussed in previous studies (Kagami 2002; 2006). The effects of the evaporation of the gas dissolved in the water packed in the spouting pipe and the loss of the evaporated gas and a part of the water during spouting have also been discussed in a previous paper (Kagami, 2009). Because the subject of this paper is the study of the effects of various shapes and their repeats in an underground watercourse, in the following numerical simulation results, we give values of parameters as if no spouting occurs and the oscillation of the height of the water pole occurs in the deep underground region.

3.1 The former models

To begin, we show the results of numerical simulation of the former extended dynamic model (Kagami, in press). In this, the temporal variation at the top of a water pole depends on the ratio of D_2 : D_1, that is, D_2/D_1 as shown in Figure 5. Corresponding values of f_{sc} and f_{se} in the case of each D_2 : D_1 are shown in Table 1. We can see that the larger the ratio of D_2 : D_1, the shorter the period of height's oscillation.

Table 1. Corresponding values of f_{sc} and f_{se} for each D_2: D_1

D_2 : D_1	f_{sc}	f_{se}
0.7	0.29	0.26
0.5	0.43	0.56
0.3	0.49	0.82

We can also observe that the larger the ratio of D_2 : D_1, the larger the amplitude of the height's oscillation. These two tendencies occur because the smaller the ratio of D_2 : D_1, the larger the values of f_{sc} and f_{se}. Consequently, the effects of the resistance are larger and hinder the water flow more in the case of a larger D_2/D_1. However, we can also observe that though the change of the height's oscillation depends on the ratio of D_2 : D_1, the change is not large. From these results, it may be concluded that the effects of only one pair of sudden expansions and contractions in an underground watercourse are not very large.

3.2 The case where there are several pairs of sudden contractions and expansions in a watercourse

Next we show the results of numerical simulation in the case where repeat pairs of sudden contractions and expansions exist in a watercourse. We adopt 0.7 as the value of D_2 : D_1. Temporal variation of a top of a water pole depends on the number of pairs of sudden expansions and contractions as shown in Figure 6. We can see from Figure 6 that the larger the number of sudden expansions and contractions, the smaller the amplitude of the height's oscillation. This is because the resistance due to pairs of sudden expansions and contractions increases in proportion to an increase in their number.

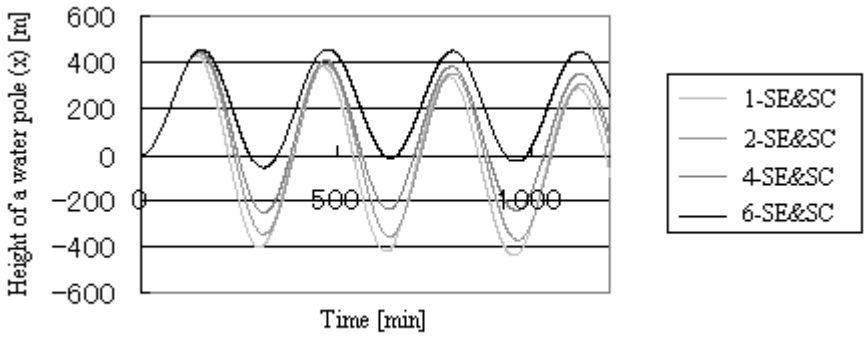

Figure 6. Temporal variation at the top of a water pole depends on the number of pairs of sudden expansions and contractions

We can also observe that the larger the number of pairs of sudden expansions and contractions, the larger the degree of transformation of the temporal variation graph. That is, the time-variation of the amplitude of the height's oscillation and so on do not always regularly change due to the number of pairs of sudden expansions and contractions. This may be the key to understanding the spouting mechanism of an irregularly spouting geyser.

As a result, though in the case of only one pair of sudden expansions and contractions, the effects are not very large, in the case of many of these pairs or the existence of complicated shapes in the underground watercourse,

the effects are not negligible.

3.3 The case where an elbow shape exists in a watercourse

In this section, we present the results of numerical simulation in the case where an elbow shape exists in a watercourse. Here the temporal variation at the top of a water pole depending on the angle of elbow is shown in Figure 7. We can see from Figure 7 that the larger the angle of elbow, the smaller the amplitude of the height's oscillation because the larger the angle of elbow, the larger the value of f_b. That is, the resistance due to an elbow shape increases in obedience to Equation (14) according to the increase in the elbow's angle.

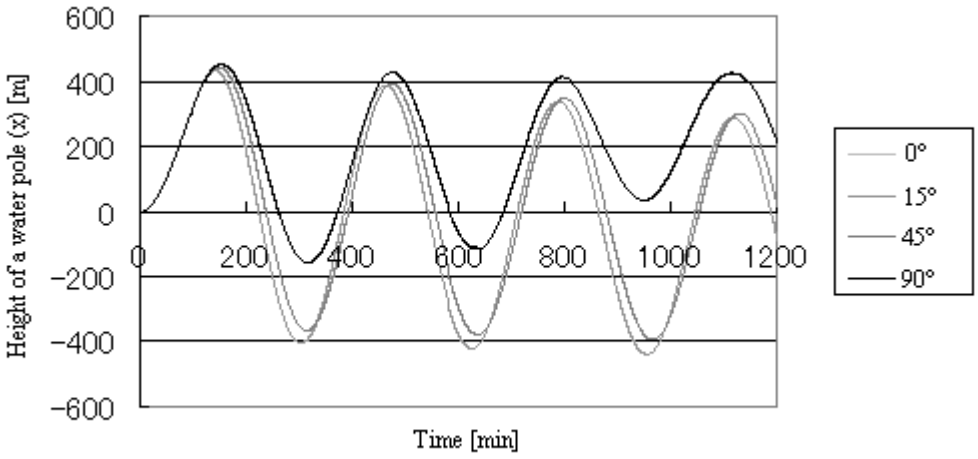

Figure 7. Temporal variation at the top of a water pole depends on the elbow's angle

We can also see that the larger the angle of elbow, the larger the degree of transformation in the temporal variation graph. Moreover, the degree of transformation in the temporal variation graph is very large in the case where the angle of elbow is sufficiently large. As a result, we can see that where there is a large angle elbow in an underground watercourse, the effects of this elbow are not negligible.

4 CONCLUSION

We modified our extended dynamic model of a geyser influenced by an inflow of gas by observing through numerical simulations the effects of an elbow shape or repeats of pairs of sudden expansions and sudden contractions in the watercourse during spouting. Through comparing the results of these numerical simulations, we conclude that a large number of pairs of sudden expansions and contractions or a large elbow angle in the underground watercourse affect greatly the geyser's spouting dynamics. Through this study, we can conjecture that shapes having a large loss water head and their repeats in an underground watercourse generally have a great affect on the spouting dynamics of a geyser.

5 REFERENCES

Honda, K. & Terada, T. (1906) *Publ. Earthq. Inv. Com.*, Vol. 22B, 51.

Husen, S. et al. (2004) *Geology*, Vol. 32, No. 6, 537.

Ishii, E. et al. (1999) *Abstracts of The 52th Annual Meeting of the Balneological Society of Japan* (pp. 28), Kusatsu, Japan.

Iwasaki, I. (1962) *Bull. Tokyo Institute of Technology*, No.46, 1.

Kagami, H. et al. (2000) *Abstracts of The 53th Annual Meeting of the Balneological Society of Japan* (pp. 27), Kotohira, Japan.

Kagami, H. (2002) *Abstracts of The 55th Annual Meeting of the Balneological Society of Japan* (pp. 33), Gero, Japan.

Kagami, H. (2003) *Proceedings of The 38th Conference of Sciete Internationale des Techniques Hydrothermales and The 56th Annual Meeting of the Balneological Society of Japan* (pp. 55-60), Beppu, Japan.

Kagami, H. (2006) *Advances in Geosciences Vol. 4: Hydrological Science*, 191.

Kagami, H. (2007) *Advances in Geosciences Vol. 6: Hydrological Science*, 203.

Kagami, H. (2007) *The 2003 IUGG General Assembly* (HW04/09P/C31-004), Perugia, Italy.

Kagami, H. (2008) *The Asia Oceania Geosciences Society's 5th Annual General Meeting* (HS01-A034), Busan, Korea.

Kagami, H., (2009) *Advances in Geosciences Vol.11: Hydrological Science*, 37.

Kagami, H. (in press) *Advances in Geosciences 2008: Hydrological Sciences*.

Katase, M. et al. (1999) *Abstracts of a meeting for presenting research papers of Kanto Gakuin University College of Engineering 1999* (pp. 99-100), Yokohama, Japan.

Lorenz, Ralph D. (2002) *Icarus*, Vol. 156, Issue 1, 176.

.

6 APPENDIX

Derivation of Equation (1)

Though a detailed derivation of Equation (1) was already given in another paper (Katase et al., 1999), we show it here again for the readers' convenience.

From the results of model experiments of a geyser induced by an inflow of gas (Kagami, 2000), we understood that the beginning of a spout is made by the loss of surface tension supporting a small amount of water packed in a pipe leading to a spouting exit. That is, in the model experiments, a situation shown in Figure 8 was assumed. A spouting hole is deep and leads to a space where gas and water are supplied at a constant rate deep under the ground. Before the start of a spout, the gas pressure in the space is supported by surface tension on the lower interface between the water and the gas (and also gravity acting on the mass of a small amount of water packed in the hole (pipe) and the pressure of the atmosphere). However, when the gas pressure in the space becomes larger than a threshold, the surface tension cannot support this gas pressure. Then a small amount of water packed in the pipe leading to the spouting exit begins to move up to the exit on the ground. In the previous model, the dynamics of a small amount of water packed in the pipe was discussed.

The gas pressure in the space just before the small amount of water begins to move up to the exit on the ground is represented as p_i, where

$$p_i = p_0 + \rho g H + f_k . \tag{17}$$

p_0 represents the pressure of the atmosphere; ρ represents the density of water; g represents gravity acceleration; H represents the length of the amount of water packed in the pipe from the lower interface

between the water and the gas to the upper interface; and f_k represents the pressure from the surface tension on the lower interface between the water and gas. f_k is represented as:

$$f_k = \frac{2\sqrt{\pi}\sigma\cos\alpha}{\sqrt{S}} \quad (18)$$

where σ represents the coefficient of the surface tension; α represents the contact angle; and S represents an area of a cross section of the pipe filling up with a small amount of water.

When a small amount of water packed in the hole begins to move upward, f_k is regarded as $f_k \to 0$. If the upper direction of a vertical line is regarded as the plus direction of the x-axis, an equation of the motion of the amount of water is written as;

$$\rho SH\frac{d^2x}{dt^2} = pS - \rho gSH - p_0 S \quad (19)$$

where p represents the pressure of the gas in the underground space. Here, x is regarded as the position of the lower interface between the water and gas in the water pole, and the friction between the walls of the pipe and the water is ignored.

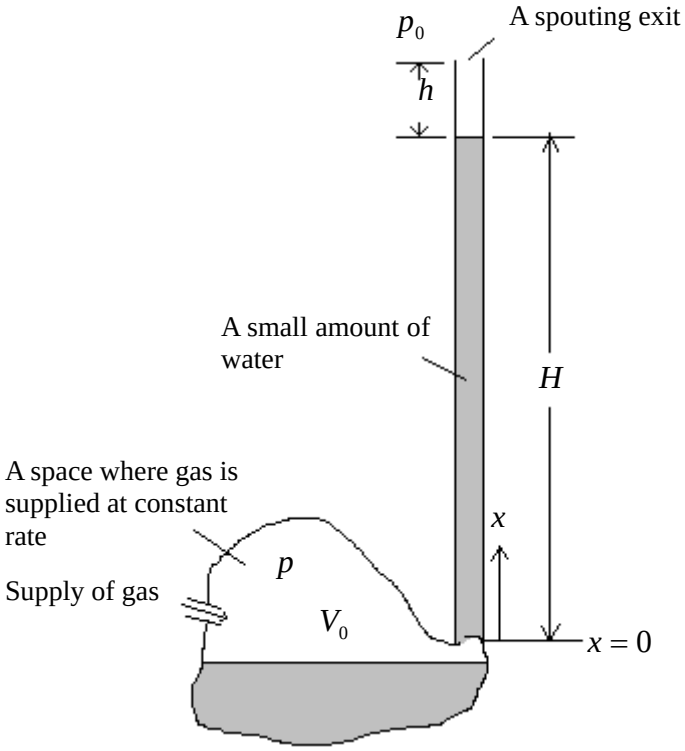

Figure 8. An illustration of a geyser induced by inflow of gas

When it is assumed that the gas in the underground space is an ideal gas and changes isothermally,

$$d\left(\frac{pV}{n}\right) = 0 \quad (20)$$

where V represents the volume of the gas filling the underground space and n represents its molar number. From Equation (20),

$$npdV + nVdp - pVdn = 0 \quad (21)$$

is derived.

When it is assumed that $x = 0$ and $V = V_0$ just before the small amount of water begins to move up, we can write V as;

$$V = V_0 + Sx \quad (22)$$

From Equation (22),

$$dV = Sdx \quad (23)$$

is derived.

From the assumption that gas is supplied at a constant rate in the underground space,

$$\frac{dn}{dt} = \beta \quad (24)$$

where β is the derived constant. From Equation (24), n can be represented as:

$$n = n_0 + \beta t \quad (25)$$

where n_0 represents the molar number when $p = p_i$ and $V = V_0$. On this account, using Equation (17), we can derive

$$n_0 = \frac{p_i V_0}{RT} = \frac{V_0}{RT}\left(p_0 + \rho g H + f_k\right) \tag{26}$$

Applying Equations (22) - (25) to Equation (21),

$$\left(n_0 + \beta t\right) pS \frac{dx}{dt} + \left(n_0 + \beta t\right)\left(V_0 + Sx\right)\frac{dp}{dt} = \left(V_0 + Sx\right)p\beta \tag{27}$$

is derived. And from Equation (19),

$$\frac{dp}{dt} = \rho H \frac{d^3 x}{dt^3} \tag{28}$$

is derived. From Equations (27) and (28) we can get

$$\left(n_0 + \beta t\right)\left(V_0 + Sx\right)\rho H \frac{d^3 x}{dt^3} + \left(n_0 + \beta t\right) pS \frac{dx}{dt} = \left(V_0 + Sx\right)p\beta \tag{29}$$

x, that is, a position in the lower interface between the water and gas in the water pole moves in obedience to Equation (29).

(Article history: Received 31 January 2009, Accepted 6 April 2010, Available online 16 April 2010)